

An Efficient Method for Solving Frequency Responses of Power-Line Networks

Bing Li*, Daniel Månsson, and Guang Yang

Abstract—This paper presents a novel approach for solving the frequency responses of a power-line network, which is a two-parallel-conductor system with multiple junctions and branches. By correcting the reflection coefficient and transmission coefficient of each junction, a complex network can be decomposed into several, single-junction, units. Based on the Baum-Liu-Tesche (BLT) equation, we preliminarily propose the calculation method of frequency responses for single-junction network. In accordance with the direction of power transfer, we calculate the frequency responses of loads connected to each junction sequentially, from the perspective of the network structure. This approach greatly simplifies the computational complexity of the network frequency responses. To verify the proposed algorithm, networks with various numbers of junctions and branches are investigated, and the results are compared with a commercial electromagnetic simulator based on the topology. The analytical results agree well with the simulated ones.

1. INTRODUCTION

For the frequency response calculation of a power-line network, Anatory et al. [1–5] gave the transfer function of power-line networks from excitation source to load responses, establishing an overall model of broadband power-line communication network with irregularly distributed branched networks, arbitrary terminal loads, various line lengths and characteristic impedances. This method gives the relationships of voltages and currents between transmitting and receiving ends, but it cannot be applied to simultaneously obtain the frequency responses at other terminal loads. Also, to take the effects of all the other loads into account, the calculation equations require to be nested for relatively more times than the method proposed in this paper.

Due to the multiple junctions in the power-line network, there are multiple reflections between junctions, which results in a multi-path propagation in the network, and the theoretical number of the propagation paths is infinite. After listing the probable propagation paths between the transmitter and receiver as much as possible, Ding and Meng [6] derived the transfer function by using a recursive model. However, it is merely suitable for the point-to-point case and the accuracy of the model depends on the selection of the number of multiple reflections. Considering the effects of the adjacent junctions, Shin et al. [7] defined a degree of distantness, where the junctions are not in the direct propagation path linking the transmitting and receiving terminals. However, the complexity of the network increases with the number of the adjacent junctions or the branches connected to the adjacent junctions, and the accuracy of the model is heavily affected by the choice of the degree of distantness. Departing from the perspective of two-port networks, Zheng et al. [8] established the power-line channel model that solves the matrix equations of the network and obtains the frequency responses of target load, by using the admittance matrix as well as the relationship between branch admittance matrix and node admittance matrix.

Received 30 January 2015, Accepted 23 April 2015, Scheduled 4 May 2015

* Corresponding author: Bing Li (libing@kth.se).

The authors are with the School of Electrical Engineering, Royal Institute of Technology KTH, Stockholm, Sweden.

Originating in the EMC community, the Baum-Liu-Tesche (BLT) equation [9–14], proposed by Baum, Liu and Tesche, can also be applied to solve this kind of problem. The equation describes the electromagnetic waves leaving and entering junctions, and the wave propagation along tubes in a transmission-line network, by using the scattering matrix and propagation matrix of the network. But the scattering parameter between two waves is difficult to obtain, as any wave is the superposition of many other waves. In addition, conventional methods do not work when facing the super matrix equations in Zheng's model [8] and the BLT model [9–14] above. Besides, a super matrix requires fairly large space for storage and its computation is time-consuming.

In our study, a more efficient approach based on the BLT equation is proposed to solve the frequency responses. The calculation results include all load frequency responses at each termination. The main idea is to divide a complex power-line network with arbitrary structure into multiple local single-junction units, instead of establishing a global model which includes the relationships between all loads. In the single-junction model, there are no multiple reflections, hence there is no need to provide any approximation on the number of reflections. By adopting a tree structure in the algorithm, all junctions and loads at the layer is simultaneously computed, in the processes of coefficients correction and frequency responses calculation, and the algorithm converges fast even if the network is fairly complex.

2. METHODS OF CALCULATING LOAD RESPONSES

In a power-line network, with the number of arbitrary distributed junctions and branches increasing, the complexity of the network increases. Different branch lengths, load values and line characteristic impedances also increase the diversity of the network configuration. In our study, with respect to various network complexities, six typical power-line networks shown in Figure 1 are investigated, and the calculation of the frequency responses at each load will be discussed subsequently in the following sections.

In this paper, \mathbf{I}_n represents the $n \times n$ identity matrix, $\mathbf{0}$ the matrix with entries 0, $\text{diag}(\ast)$ the diagonal matrix, and $\text{adiag}(\ast)$ the anti-diagonal matrix. $\Re(\ast)$ and $\Im(\ast)$ respectively denote the real part and the imaginary part of a complex number, and $(\ast)^T$ stands for transpose.

2.1. The BLT Equation

To solve the frequency responses, for the simplest power-line network (see Figure 1(a)), the BLT equation [11] is applied. Assuming that the line length is L , propagation constant is γ , characteristic impedance is Z_c , and the load impedances are Z_{L1} and Z_{L2} , respectively. The excitation source consists of a lumped voltage source V_s and a lumped current source I_s , which are located at a distance of x_s from the left load Z_{L1} (see Figure 2).

When the excitation source (V_s and I_s) act on the power-line, the voltage waves propagate along the power-line. Note that the voltage consists of the incident waves $\mathbf{V}^{\text{inc}} = [V_1^{\text{inc}}, V_2^{\text{inc}}]^T$ and the reflected waves $\mathbf{V}^{\text{ref}} = [V_1^{\text{ref}}, V_2^{\text{ref}}]^T$ shown in Figure 3, by following the BLT equation in the matrix way, we have

$$\mathbf{V}^{\text{inc}} = \mathbf{\Gamma} \mathbf{V}^{\text{ref}} + \mathbf{S}, \quad (1)$$

where $\mathbf{\Gamma} = \text{adiag}(e^{-\gamma L}, e^{-\gamma L})$. Besides, $\mathbf{S} = [S_1, S_2]^T$ in (1) represents the excitation vector, which is given by

$$\begin{bmatrix} S_1 \\ S_2 \end{bmatrix} = \begin{bmatrix} -\frac{1}{2}(V_s - Z_c I_s) e^{-\gamma x_s} \\ \frac{1}{2}(V_s + Z_c I_s) e^{-\gamma(L-x_s)} \end{bmatrix}.$$

Generally, the propagation constant $\gamma = \sqrt{j\omega\mu(\sigma + j\omega\epsilon)}$ is a complex number. Let $\alpha = \Re(\gamma)$ and $\beta = \Im(\gamma)$ be the attenuation constant and phase constant, respectively. According to [15], we have

$$\alpha = \omega \sqrt{\frac{\mu\epsilon}{2}} \left(\sqrt{1 + \left(\frac{\sigma}{\omega\epsilon}\right)^2} - 1 \right)^{1/2} \quad \text{and} \quad \beta = \omega \sqrt{\frac{\mu\epsilon}{2}} \left(\sqrt{1 + \left(\frac{\sigma}{\omega\epsilon}\right)^2} + 1 \right)^{1/2}.$$

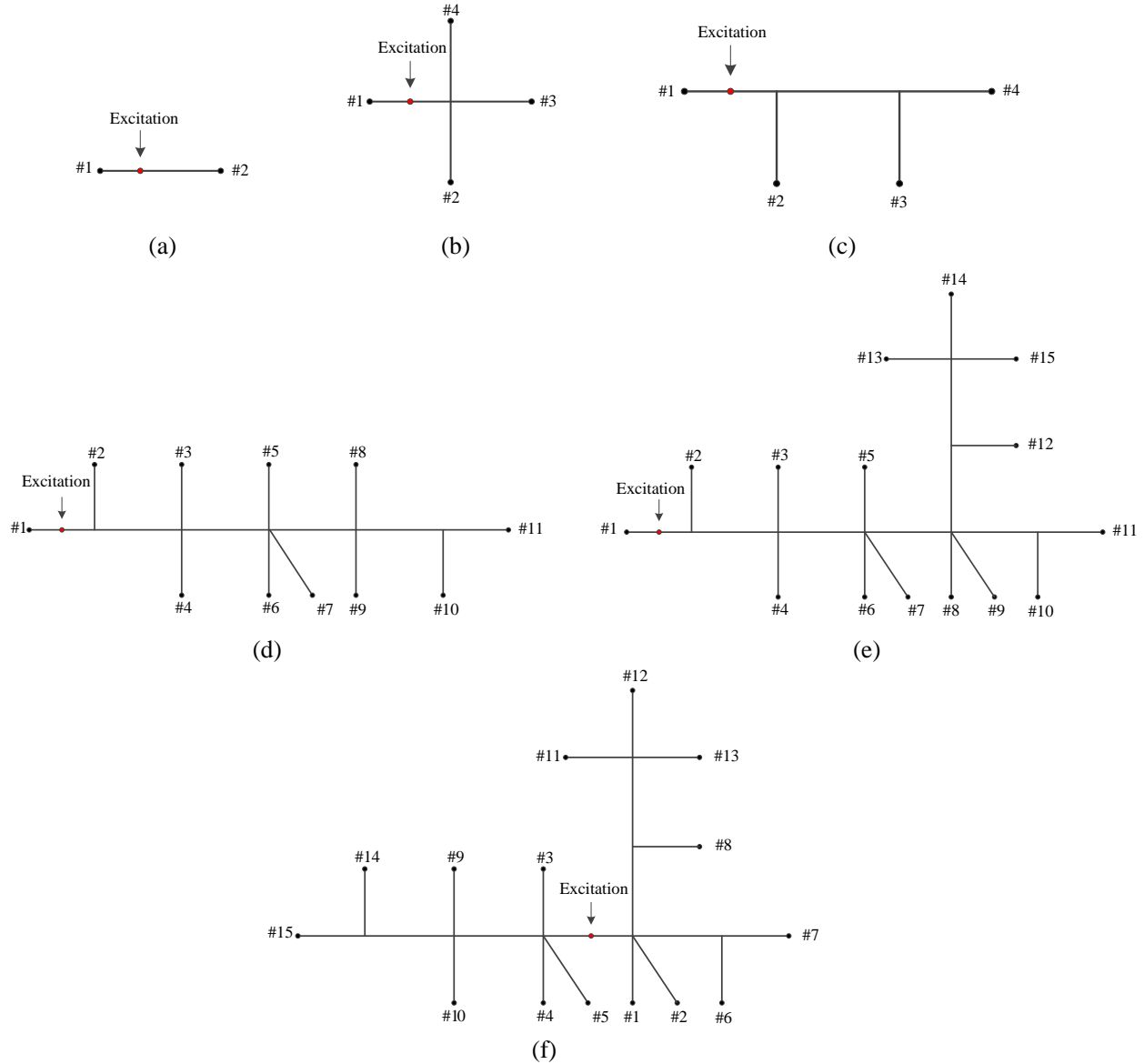


Figure 1. Different types of power-line network. (a) Two loads without junction; (b) four loads with one junction; (c) four loads with two junctions; (d) eleven loads with five junctions; (e) fifteen loads with seven junctions; and (f) fifteen loads with seven junctions with different excitation.

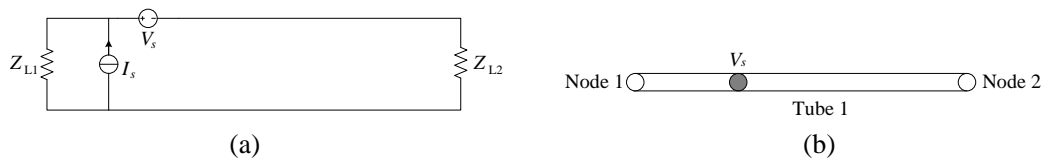


Figure 2. The network of Figure 1(a). (a) Geometry; and (b) tube model.

Here, ω is angular frequency, and μ , ϵ and σ are permeability, permittivity and conductivity of the medium between two conductors in a transmission line. Particularly, if the media is lossless, that is $\sigma = 0$, then α and β are reduced to

$$\alpha = 0 \quad \text{and} \quad \beta = \omega\sqrt{\mu\epsilon} = \frac{\omega}{v} = \frac{2\pi f}{v} = \frac{2\pi}{\lambda}, \quad (2)$$

where v is the velocity of wave and λ the wavelength.

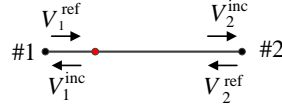


Figure 3. Voltage travelling waves on the power-line.

Following the transmission line theory, the incident voltage and reflected voltage at a load satisfies

$$V^{\text{ref}} = \rho V^{\text{inc}}, \quad (3)$$

where ρ is the reflection coefficient shown as

$$\rho = \frac{Z_L - Z_c}{Z_L + Z_c}. \quad (4)$$

Thus, in the network shown in Figure 1(a), given the reflection coefficients ρ_1 and ρ_2 at two terminals respectively, the reflected voltage can be expressed as

$$\mathbf{V}^{\text{ref}} = \mathbf{P} \mathbf{V}^{\text{inc}}, \quad (5)$$

where $\mathbf{P} = \text{diag}(\rho_1, \rho_2)$.

Note that the frequency responses $\mathbf{V} = [V_1, V_2]^T$ is the superposition of the incident and reflected voltages, say

$$\mathbf{V} = \mathbf{V}^{\text{inc}} + \mathbf{V}^{\text{ref}}, \quad (6)$$

by combining (1), (5) and (6), we finally obtain the frequency responses by

$$\mathbf{V} = (\mathbf{I}_2 + \mathbf{P})(\mathbf{I}_2 - \mathbf{G}\mathbf{P})^{-1} \mathbf{S}. \quad (7)$$

2.2. The Modified BLT Equation

In this section, we extend our case to the network with one junction and four branches, as shown in Figure 4. At the branch i , $i = 1, 2, 3, 4$, the length is L_i , the propagation constant is γ_i , and the characteristic impedances are Z_{ci} . Besides, at the end of the branch i , the load is given by Z_{Li} , which has the same index with branch. The excitation sources are located on the first branch.

Due to the junction in this network, the BLT equation needs to be modified. We suppose that TEM is the main mode of wave propagation, and if this mode is dominant also through the junction (as seen in [16]), then the reflection can be described by the transmission line theory. The voltage travelling waves propagate along all branches connected to a junction, since they are connected in parallel. The

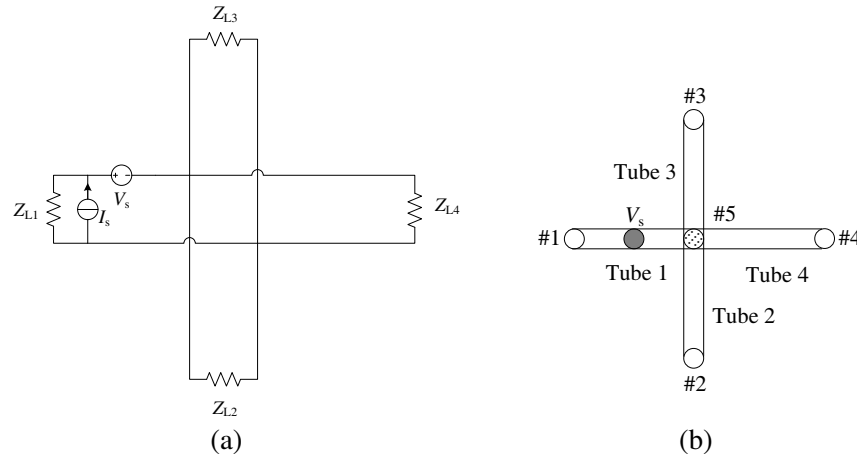


Figure 4. Specific network of Figure 1(b). (a) Geometry; and (b) tube model.

reflection coefficients $\rho^{(i)}$ and the transmission coefficients $T^{(i)}$ for each branch at the junction, where the superscript i corresponds to the branch i , are respectively given by

$$\left\{ \begin{array}{l} \rho^{(1)} = \frac{Z_{c2} \parallel Z_{c3} \parallel Z_{c4} - Z_{c1}}{Z_{c2} \parallel Z_{c3} \parallel Z_{c4} + Z_{c1}} \\ \rho^{(2)} = \frac{Z_{c1} \parallel Z_{c3} \parallel Z_{c4} - Z_{c2}}{Z_{c1} \parallel Z_{c3} \parallel Z_{c4} + Z_{c2}} \\ \rho^{(3)} = \frac{Z_{c1} \parallel Z_{c2} \parallel Z_{c4} - Z_{c3}}{Z_{c1} \parallel Z_{c2} \parallel Z_{c4} + Z_{c3}} \\ \rho^{(4)} = \frac{Z_{c1} \parallel Z_{c2} \parallel Z_{c3} - Z_{c4}}{Z_{c1} \parallel Z_{c2} \parallel Z_{c3} + Z_{c4}} \end{array} \right. \quad \text{and} \quad \left\{ \begin{array}{l} T^{(1)} = 1 + \rho^{(1)} \\ T^{(2)} = 1 + \rho^{(2)} \\ T^{(3)} = 1 + \rho^{(3)} \\ T^{(4)} = 1 + \rho^{(4)} \end{array} \right. , \quad (8)$$

Note that, for n parallel-connected power line with characteristic impedance Z_k , $k = 1, 2, \dots, n$, we have

$$Z_1 \parallel Z_2 \parallel \dots \parallel Z_n = \left(\sum_{k=1}^n Z_k^{-1} \right)^{-1}, \quad (9)$$

without loss of generality, for any $i \in \{1, 2, 3, 4\}$, the reflection coefficients and transmission coefficients in (8) can be formulated as

$$\rho^{(i)} = \frac{\left(\sum_{j \neq i} Z_{cj}^{-1} \right)^{-1} - Z_{ci}}{\left(\sum_{j \neq i} Z_{cj}^{-1} \right)^{-1} + Z_{ci}} \quad \text{and} \quad T^{(i)} = 1 + \rho^{(i)}. \quad (10)$$

Particularly, if the branches have the identical characteristic impedance, say $Z_{ci} = Z_c$, $i = 1, 2, 3, 4$, the reflection coefficient $\rho^{(i)}$ at each branch can be reduced to

$$\rho^{(i)} = \frac{Z_c/3 - Z_c}{Z_c/3 + Z_c} = -\frac{1}{2}. \quad (11)$$

Based on the reflection coefficient and the transmission coefficient at the junction, we modify the original BLT equation. Similar to the analysis in Section 2.1, for the voltage travelling waves shown in Figure 5, we have the relationship between the incident voltages and the reflected as shown in (1), with $\mathbf{V}^{\text{inc}} = [V_1^{\text{inc}}, V_2^{\text{inc}}, V_3^{\text{inc}}, V_4^{\text{inc}}]^T$, $\mathbf{V}^{\text{ref}} = [V_1^{\text{ref}}, V_2^{\text{ref}}, V_3^{\text{ref}}, V_4^{\text{ref}}]^T$, the transmission matrix

$$\mathbf{\Gamma} = \begin{bmatrix} \rho^{(1)} e^{-2\gamma_1 L_1} & T^{(2)} e^{-(\gamma_1 L_1 + \gamma_2 L_2)} & T^{(3)} e^{-(\gamma_1 L_1 + \gamma_3 L_3)} & T^{(4)} e^{-(\gamma_1 L_1 + \gamma_4 L_4)} \\ T^{(1)} e^{-(\gamma_1 L_1 + \gamma_2 L_2)} & \rho^{(2)} e^{-2\gamma_2 L_2} & T^{(3)} e^{-(\gamma_2 L_2 + \gamma_3 L_3)} & T^{(4)} e^{-(\gamma_2 L_2 + \gamma_4 L_4)} \\ T^{(1)} e^{-(\gamma_1 L_1 + \gamma_3 L_3)} & T^{(2)} e^{-(\gamma_2 L_2 + \gamma_3 L_3)} & \rho^{(3)} e^{-2\gamma_3 L_3} & T^{(4)} e^{-(\gamma_3 L_3 + \gamma_4 L_4)} \\ T^{(1)} e^{-(\gamma_1 L_1 + \gamma_4 L_4)} & T^{(2)} e^{-(\gamma_2 L_2 + \gamma_4 L_4)} & T^{(3)} e^{-(\gamma_3 L_3 + \gamma_4 L_4)} & \rho^{(4)} e^{-2\gamma_4 L_4} \end{bmatrix}, \quad (12)$$

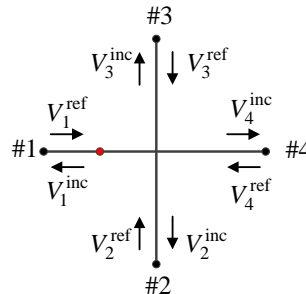


Figure 5. Voltage travelling waves in the network of Figure 1(b).

and the excitation vector

$$\mathbf{S} = \begin{bmatrix} S_1 \\ S_2 \\ S_3 \\ S_4 \end{bmatrix} = \begin{bmatrix} -\frac{1}{2}(V_s - Z_c I_s)e^{-\gamma_1 x_s} + \rho^{(1)} \cdot \frac{1}{2}(V_s + Z_c I_s)e^{-\gamma_1(2L_1 - x_s)} \\ T^{(1)} \cdot \frac{1}{2}(V_s + Z_c I_s)e^{-(\gamma_1(L_1 - x_s) + \gamma_2 L_2)} \\ T^{(1)} \cdot \frac{1}{2}(V_s + Z_c I_s)e^{-(\gamma_1(L_1 - x_s) + \gamma_3 L_3)} \\ T^{(1)} \cdot \frac{1}{2}(V_s + Z_c I_s)e^{-(\gamma_1(L_1 - x_s) + \gamma_4 L_4)} \end{bmatrix}. \quad (13)$$

Additionally, given the reflection coefficient ρ_i at the terminal i , $i = 1, 2, 3, 4$, we have

$$\mathbf{P} = \text{diag}(\rho_1, \rho_2, \rho_3, \rho_4). \quad (14)$$

Following the relationships for the reflected and incident waves in (1) and (5), as well as the superposition law in (6), we similarly obtain the frequency response matrix $\mathbf{V} = [V_1, V_2, V_3, V_4]^T$ as

$$\mathbf{V} = (\mathbf{I}_4 + \mathbf{P})(\mathbf{I}_4 - \mathbf{TP})^{-1} \mathbf{S}. \quad (15)$$

Comparing (15) with (7), we can easily find that they have the same form of expression, but with completely different matrices (vectors).

3. UNIT CALCULATION METHOD BASED ON COEFFICIENT CORRECTION

Here, a power-line network with multiple junctions is discussed. We take the network with two junctions and four branches (loads) as an example and conduct the analysis, and subsequently develop an algorithm for computing multiple distributed junctions and branches. Within the network shown in Figure 1(c), we assume the branch lengths, propagation constants, characteristic impedances and load values are distinct. The excitation source is still located on the first branch. Besides, the length of the line between the two junctions is L .

The algorithm idea consists of two steps. We first divide the network into two single-junction network units, as shown in Figure 6. The cut is located at the second junction, and the equivalent

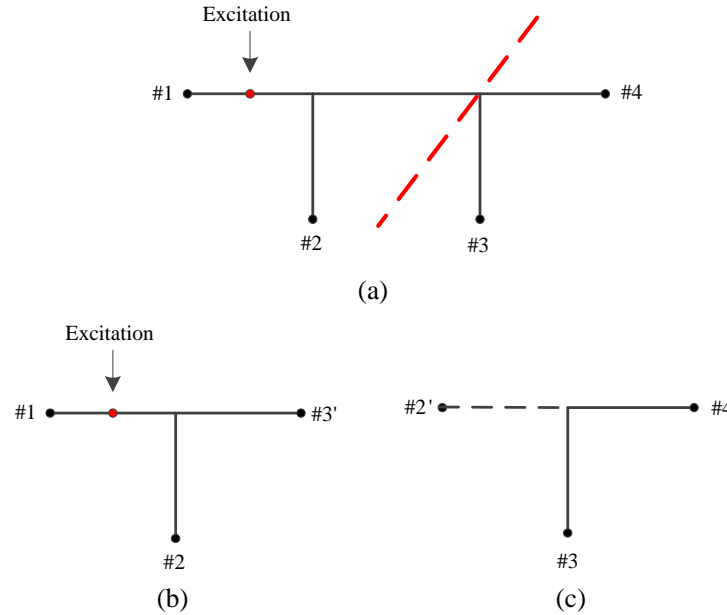


Figure 6. The divided two-junction network. (a) Dividing point; (b) the first unit with excitation source; and (c) the second unit with a virtual branch of zero length.

loads in two units are labelled as $3'$ and $2'$, respectively. To hold the structure of the second unit, i.e., ensure that there are still three branches connected to the junction, a virtual branch of length zero is introduced to the second junction. For the single-junction network shown in Figure 6(b), we use the modified BLT equation to solve the load responses. Afterwards, according to the transfer direction of power, the power absorbed by the load $3'$ is put as the excitation source of the second single-junction network, and compute the load responses in the second unit. More details are provided in the following parts.

3.1. Coefficient Correction

To calculate the frequency responses of the first unit, the reflection coefficient and the transmission coefficient are required. At the second junction of the network shown in Figure 6(a), the coefficients can be obtained by using (8). To take the circled part shown in Figure 7 as a super load, the effects of load 3 and load 4 need to be taken into account.

For the super load, we set $\mathbf{S} = \mathbf{0}$ since no excitation source participates. Considering the length of the virtual branch is zero, by applying (12), we obtain

$$\begin{bmatrix} V_{3'}^{\text{ref}} \\ V_3^{\text{inc}} \\ V_4^{\text{inc}} \end{bmatrix} = \begin{bmatrix} T_2 - 1 & T_2^{(3)} e^{-\gamma_3 L_3} & T_2^{(4)} e^{-\gamma_4 L_4} \\ T_2 e^{-\gamma_3 L_3} & \rho_2^{(3)} e^{-2\gamma_3 L_3} & T_2^{(4)} e^{-(\gamma_3 L_3 + \gamma_4 L_4)} \\ T_2 e^{-\gamma_4 L_4} & T_2^{(3)} e^{-(\gamma_3 L_3 + \gamma_4 L_4)} & \rho_2^{(4)} e^{-2\gamma_4 L_4} \end{bmatrix} \begin{bmatrix} V_{3'}^{\text{inc}} \\ V_3^{\text{ref}} \\ V_4^{\text{ref}} \end{bmatrix}, \quad (16)$$

where $\rho_2^{(3)}, \rho_2^{(4)}$ are the reflection coefficients, and $T_2, T_2^{(3)}, T_2^{(4)}$ are the transmission coefficients at the second junction for the connected line and two branches. The superscript represents the branch index and the subscript is junction number.

Besides, by following the definition of reflection coefficient, we have

$$\begin{bmatrix} V_3^{\text{ref}} \\ V_4^{\text{ref}} \end{bmatrix} = \begin{bmatrix} \rho_3 & 0 \\ 0 & \rho_4 \end{bmatrix} \begin{bmatrix} V_3^{\text{inc}} \\ V_4^{\text{inc}} \end{bmatrix}, \quad (17)$$

where ρ_3 and ρ_4 are the reflection coefficients at load 3 and 4, respectively. Substituting (17) into (16), the corrected reflection coefficient for the load $3'$ is derived as

$$\rho_{3'} \triangleq \frac{V_{3'}^{\text{ref}}}{V_{3'}^{\text{inc}}} = (T_2 - 1) + \frac{T_2 T_2^{(3)}}{A \left(1 - \left(\frac{T_2^{(3)}}{A} + \frac{T_2^{(4)}}{B} \right) \right)} + \frac{T_2 T_2^{(4)}}{B \left(1 - \left(\frac{T_2^{(3)}}{A} + \frac{T_2^{(4)}}{B} \right) \right)}, \quad (18)$$

where $A = 1 + \frac{1}{\rho_3 e^{-2\gamma_3 L_3}}, B = 1 + \frac{1}{\rho_4 e^{-2\gamma_4 L_4}}$. From (18), we can see that the calculation of the reflection coefficient for the super load $3'$ involves the terminal load reflection coefficients, propagation constants, branch lengths and branch transmission coefficients.

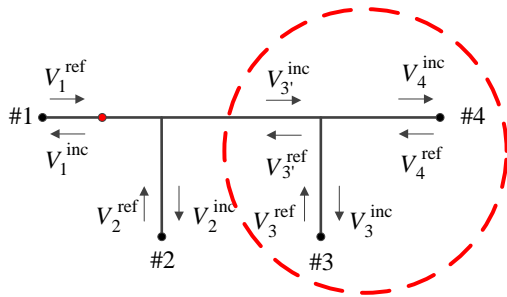


Figure 7. Voltage travelling waves in the network of Figure 1(c).

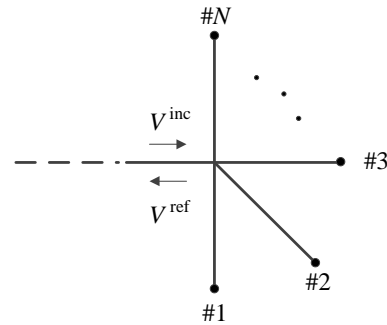


Figure 8. Single-junction network with $N + 1$ branches.

Without loss of generality, for the junction with $N+1$ branches, as shown in Figure 8, the corrected coefficient at the junction is

$$\rho' = (T - 1) + \frac{T \left(\frac{T^{(1)}}{A_1} + \frac{T^{(2)}}{A_2} + \dots + \frac{T^{(N)}}{A_N} \right)}{1 - \left(\frac{T^{(1)}}{A_1} + \frac{T^{(2)}}{A_2} + \dots + \frac{T^{(N)}}{A_N} \right)} = T \left(1 - \sum_{i=1}^N \frac{T^{(i)}}{A_i} \right)^{-1} - 1 = T' - 1, \quad (19)$$

where $A_i = 1 + \frac{1}{\rho_i e^{-2\gamma_i L_i}}$, $T^{(i)}$ is the transmission coefficients for branch i , and T denotes the transmission coefficient for the connected line. Here, T' is regarded as the equivalent transmission coefficient, from the angle of the connected line to characterize the single-junction unit.

3.2. Calculation of Frequency Response at Each Load

The calculation of the frequency response at each load runs recursively. In our specific model, since we decompose the network into two units, we should first solve the unit one, regarding the load 1, 2 and 3'. After obtaining the frequency response at load 3', we access the unit two to compute the frequency responses of the loads in unit two.

(1) *For Unit One:* there are three branches connected to the junction. Supposing that the value of the super load 3' is $Z_{L3'}$, the equivalent model is shown in Figure 9. By applying the modified BLT approach proposed in Section 2.2, we obtain the frequency responses at the three loads.

(2) *For Unit Two:* we use the frequency responses of load 3' as excitation source, as shown in Figure 10(a). Since $V_{3'}$ is a voltage determined by Unit One, the symbol of the controlled voltage source is used here. The length of the virtual branch where the excitation source are placed is set to zero. To apply the modified BLT equation, we construct a network similar to the one shown in Figure 4(a). Therefore, the location of the excitation source shifts to the place x_s away from the terminal. Because the length of the virtual branch is zero, the value of x_s should also be zero. In addition, to show the integrity of analysis, technically we add an equivalent controlled current source (see Figure 10(b)) at the same position of the controlled voltage source, but the value of the current should be zero. Considering that the terminal of the virtual branch is shorted, a virtual load, $Z_{L2'}$, is added at the terminal, as shown in Figure 10(b), and the load value is zero. According to (4), the reflection coefficient is set to be $\rho_{2'} = -1$. Then, the frequency responses of the loads in unit two are obtained. So far, all load frequency responses in the entire network are solved.

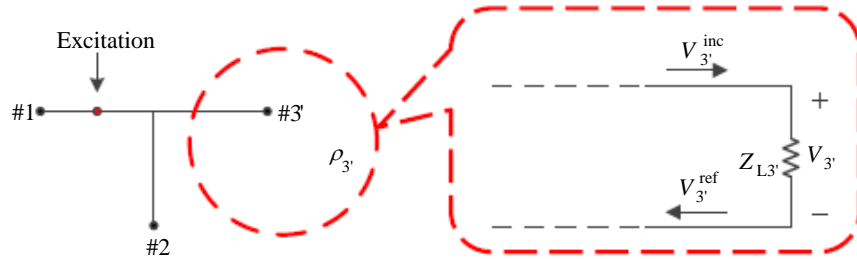


Figure 9. Equivalent model of the super load.

4. ALGORITHM

In this section we first describe the principle, which is followed by its complexity analysis. In the complexity analysis part, we compare with two other related methods, and we show that our proposed algorithm is more efficient.

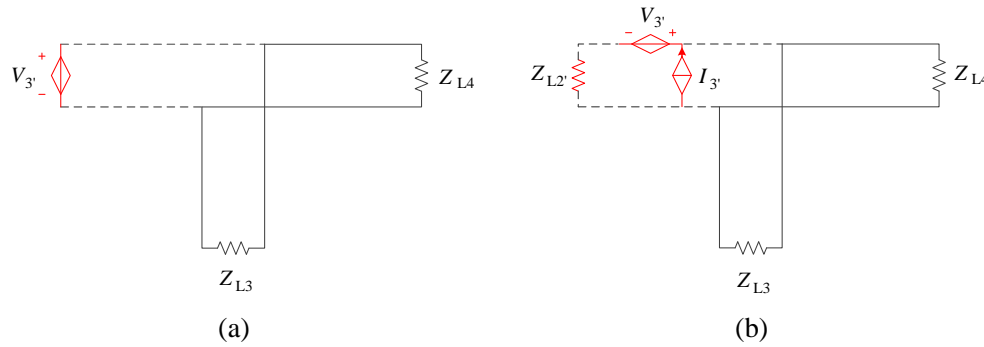


Figure 10. The second unit of the network. (a) The second unit with equivalent excitation source; and (b) deformation of the second unit.

4.1. Algorithm Description

In what follows, we develop an algorithm that is applied to the complex power-line networks with multiple distributed junctions and branches, such as the networks in Figure 1(e) and Figure 1(f), aiming at computing the frequency response in an efficient way.

Taking the network in Figure 1(e) as an example, there are three main branches, seven junctions and fifteen branches with loads. It is evident that the network is tree-structured and can be displayed in the topology given by Figure 11. The junction that connects to the excitation source is placed at the top point, and is set to be root node of the tree. Throughout the tree, there are totally seven layers, which is one more than the height of the tree.

Given that we have the knowledge of all load values, branch lengths, junctions and the excitation

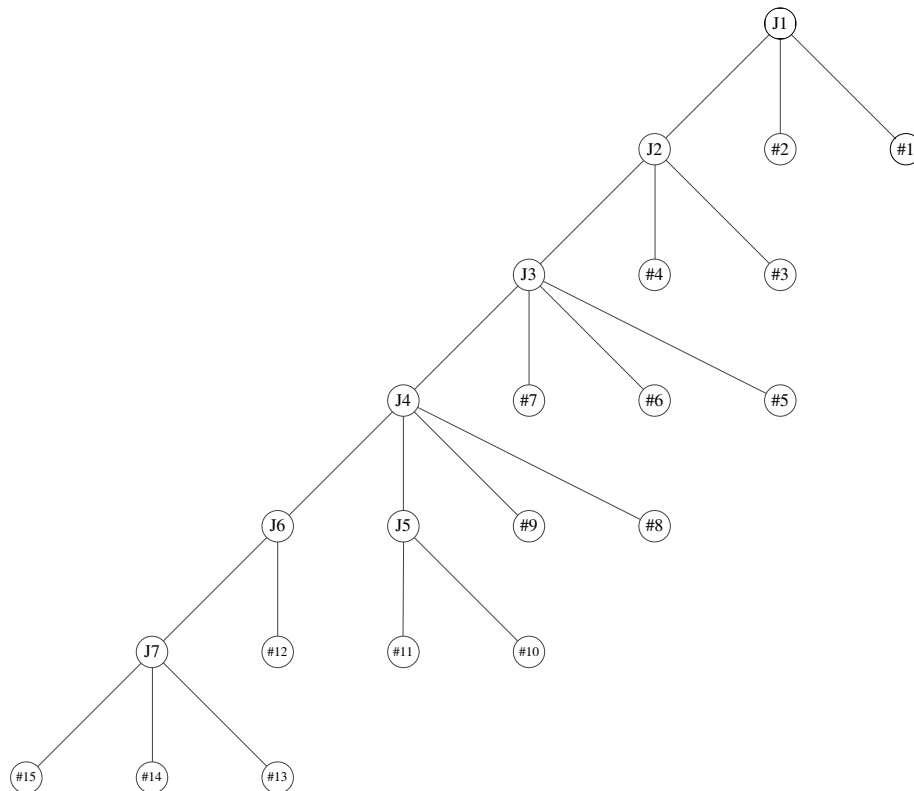


Figure 11. Tree structure of the network shown in Figure 1(e).

source, the algorithm consists of two phases and the main steps are outlined as follows:

- (i) *From the bottom to the top*: recursively correct the reflection coefficient at junctions on the upper layer until the root (top point) is reached;
- (ii) *From the top to the bottom*: after correcting all the reflection coefficients, recursively calculate the load response for the associated child nodes until the bottom layer is reached.

For a tree-structured network with n layers, the procedure of the algorithm is illustrated in Figure 12.

4.2. Algorithm Complexity Analysis

Given a tree-structure network of height n , equivalently $n + 1$ layers, we denote by \mathcal{X}_i , $i = 1, 2, \dots, n$, the set of child nodes number for the parents at layer i . To be more precise, at layer i , assuming there are l_i parents, then \mathcal{X}_i is shown as

$$\mathcal{X}_i = \{X_{i,1}, X_{i,2}, \dots, X_{i,l_i}\}, \quad (20)$$

where $X_{i,k}$, $k = 1, 2, \dots, l_i$, corresponds to the number of child nodes for the k th parent at layer i .

To quantify the algorithm efficiency, a straightforward and effective way is to count the number of arithmetic operations (i.e., the addition and multiplication) when conducting the calculation. Based on the complexity metric given above, we analyze the efficiency performance of the following three methods: our proposed method, the recursive time domain method [6], and simulations made with the numerical software, EMEC [17]. As we will discuss, those three schemes are all involving the matrix inversion, which contributes most among all possible operations in terms of the computational complexity.

Although the time complexity of matrix inversion can be improved through designing related algorithms (as stated in [18, 19], the steps of arithmetic operations of inversion or multiplication for a matrix of order m are bounded by $\mathcal{O}(m^w)$, where $2 < w \leq 3$ is determined by the algorithms. Here, the notation $\mathcal{O}(\ast)$ describes the limiting behaviour of a function when the argument tends towards a particular value or infinity, which is widely used in time complexity analysis to classify algorithms [20, 21]), we here take the *Gaussian-Jordan* elimination method for matrix inversion as

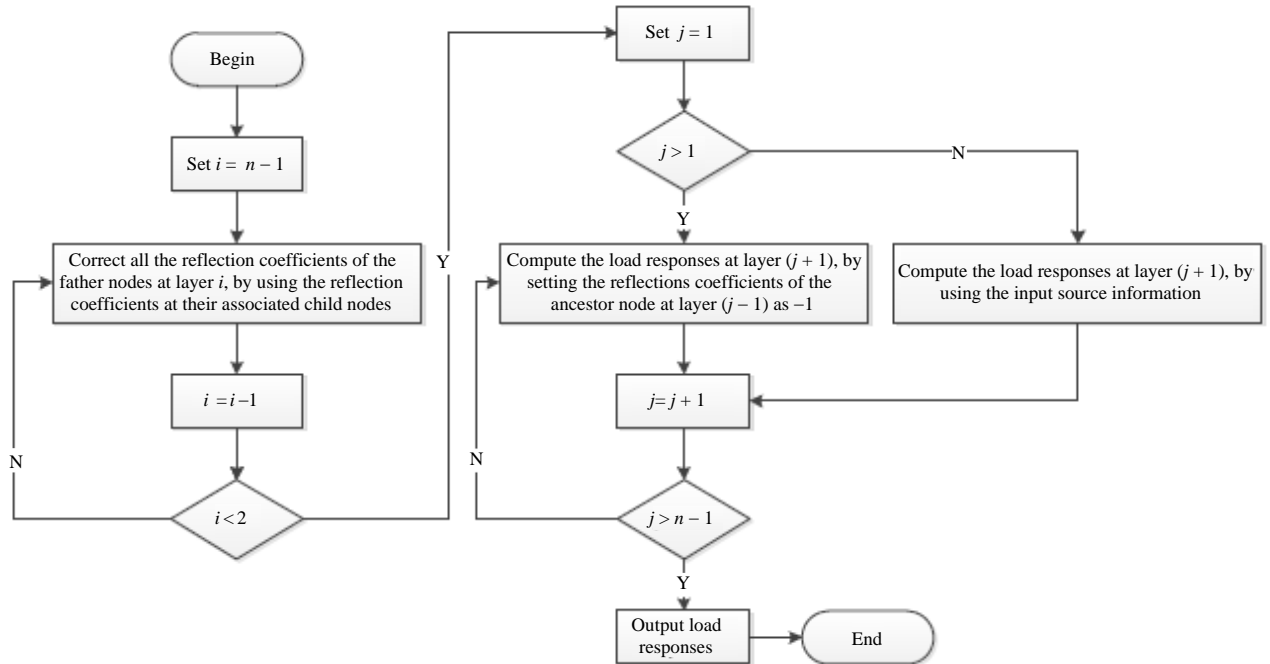


Figure 12. Flow chart of the algorithm.

the standard approach to obtain the matrix inversion, whose number of arithmetic operations can be expressed [22] as $f(N) = \sum_{k=1}^3 a_k N^k$, where a_k , $k = 1, 2, 3$, are certain scalars such that $f(N)$ is monotonically increasing with N , and N is the order of matrix. Commonly, we consider the worst case to test the complexity of algorithm, then the numbers of additions and multiplications are respectively given by [23]

$$f_A(N) = \frac{1}{3}N^3 + \frac{1}{2}N^2 - \frac{5}{6}N \quad \text{and} \quad f_M(N) = \frac{1}{3}N^3 + N^2 + \frac{1}{3}N, \quad (21)$$

thus the total operations is

$$f(N) \triangleq f_A(N) + f_M(N) = \frac{2}{3}N^3 + \frac{3}{2}N^2 - \frac{1}{2}N \approx \tilde{f}(N) \triangleq \frac{2}{3}N^3, \quad \text{for } N \gg 1. \quad (22)$$

where $\tilde{f}(N)$ is an approximation of $f(N)$ for sufficiently large N . For the sake of simplicity, in the following analysis, we adopt the metric $\tilde{f}(\cdot)$ to evaluate the complexity.

- In our proposed algorithm, we assume each parent node has the capability of processing data locally, individually, then the total number of operations \mathcal{M}_1 is given by:

$$\mathcal{M}_1 = 2 \sum_{i=1}^n \sum_{j=1}^{l_i} f(X_{i,j}) \approx 2 \sum_{i=1}^n \sum_{j=1}^{l_i} \tilde{f}(X_{i,j}) = \frac{4}{3} \sum_{i=1}^n \sum_{j=1}^{l_i} X_{i,j}^3 \quad (23)$$

where the factor 2 comes from the round-trip procedure, i.e., from bottom to top, then back to bottom.

- By the recursive time domain solution proposed in [6], we need to establish a global $N \times N$ matrix \mathbf{A} to represent the reflection/transmission coefficients, and the order N is twice of edges in the tree graph, say

$$N = 2m = 2 \sum_{i=1}^n \sum_{j=1}^{l_i} X_j^{(i)}. \quad (24)$$

Note that the recursive time domain solution involves the multipath, strictly speaking, to achieve the perfect ideal theoretical results of load responses, we should consider all potential paths. In graph theory and matrix theory, we follow the concept of transition matrix to verify if the destination is reachable after several transitions. To be more precise, in [6], the reflection/transmission matrix coefficient matrix \mathbf{A} is the transition matrix, and the following operation to calculate the frequency response value is recursively multiplying \mathbf{A} and conducting the superposition on the derived values of each iteration. Equivalently, the manipulation can be summarized by

$$\lim_{K \rightarrow \infty} \sum_{i=0}^K \mathbf{A}^i = \mathbf{I}_N + \mathbf{A} + \mathbf{A}^2 + \cdots = (\mathbf{I}_N - \mathbf{A})^{-1}, \quad (25)$$

where K is referred to as the iterations, \mathbf{I}_N is an identity matrix of size N . It is easy to see, the above closed-form expression derives the load response with perfect precision. In this manner, the

$$\mathcal{M}_2 \approx \tilde{f}(N) = \frac{2}{3} \left(2 \sum_{i=1}^n \sum_{j=1}^{l_i} X_{i,j} \right)^3 > \frac{16}{3} \sum_{i=1}^n \left(\sum_{j=1}^{l_i} X_{i,j} \right)^3 > \frac{16}{3} \sum_{i=1}^n \sum_{j=1}^{l_i} X_{i,j}^3 \approx 4\mathcal{M}_1 \quad (26)$$

- In the software EMEC, nodal analysis is used. The employed algorithm is based on the admittance matrix for the whole network, which is inverted into a system impedance matrix, and the voltage in all nodes is calculated by multiplying the impedance with the current vector [17]. Note that, the order of the admittance matrix is the number of all nodes (including the root node), thus, following the previous notations, we have the $N \times N$ admittance matrix with

$$N = m + 1 = \sum_{i=1}^n \sum_{j=1}^{l_i} X_j^{(i)} + 1, \quad (27)$$

it is easy to show that, the metric \mathcal{M}_3 satisfies

$$\mathcal{M}_1 < \mathcal{M}_3 \approx \tilde{f}(N) = \frac{2}{3} \left(1 + \sum_{i=1}^n \sum_{j=1}^{l_i} X_{i,j} \right)^3 < \mathcal{M}_2 \quad (28)$$

In light of above analysis, we observe, for the distributed calculation methods (i.e., the first scheme), the complexity merely relies on the maximum degree of the tree graph, however, the subsequent two algorithms require the sum of all degrees. Obviously, given the fixed height of tree-structured network n , by increasing the number of loads, we can see that, $\mathcal{M}_1 \ll \mathcal{M}_3 < \mathcal{M}_2$, which implies the significant improvement in efficiency.

5. COMPARISON OF CALCULATING RESULTS

To validate the algorithm, we take the commercial software EMEC [17] as the benchmark, which is based on electromagnetic topology. For test purpose, the parameters chosen for the variables in the power-line networks are given in Table 1–Table 5. The characteristic impedances for each power line are all 45Ω , which are consistent with the cable data given in the datasheet of the software EMEC.

Table 1. Parameters for the network shown in Figure 1(a).

Parameter	Load (Ω)		Length (m)	Distance (m)	Voltage (V)	Current (A)
	Z_{L1}	Z_{L2}	L	x_s	V_s	I_s
Value	200	400	10	1	100	0

Table 2. Parameters for the network shown in Figure 1(b).

Parameter	Load (Ω)				Length (m)				Distance (m)	Voltage (V)	Current (A)
	Z_{L1}	Z_{L2}	Z_{L3}	Z_{L4}	BL_1	BL_2	BL_3	BL_4	x_s	V_s	I_s
Value	10	10	100	200	10	10	10	10	5	100	0

Table 3. Parameters for the network shown in Figure 1(c).

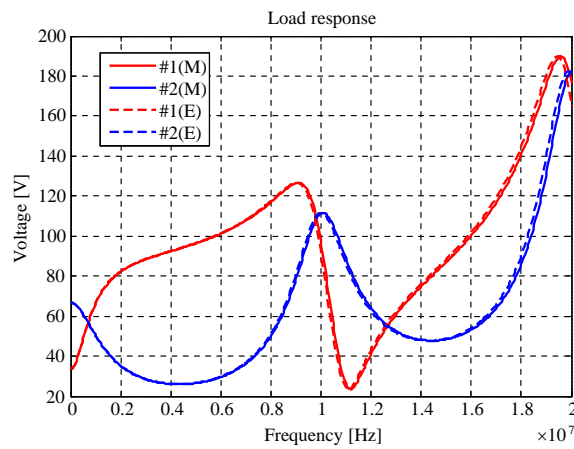
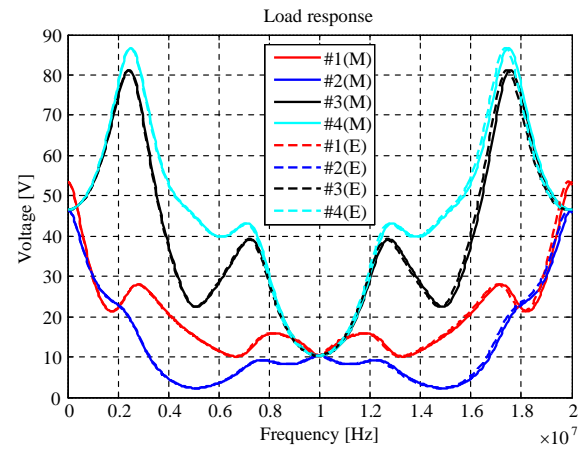
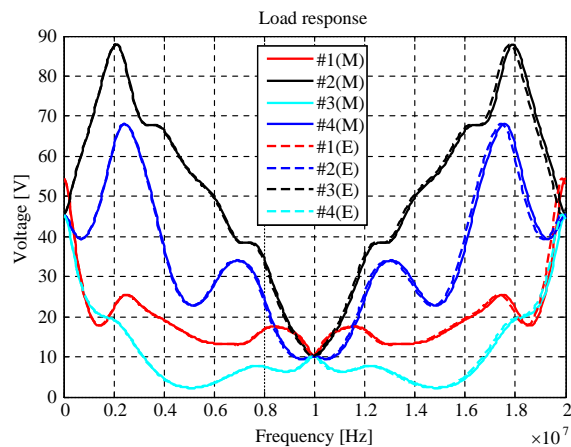
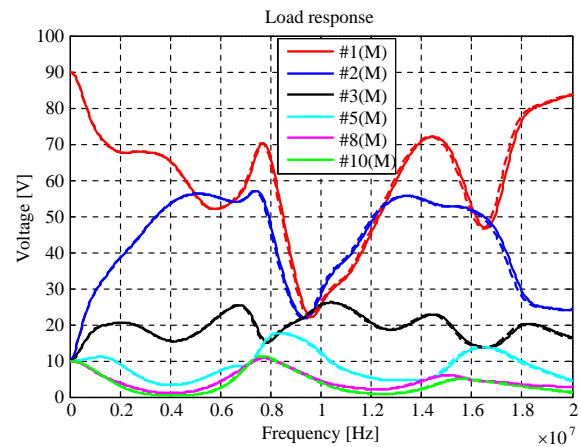
Parameter	Load (Ω)				Length (m)					Distance (m)	Voltage (V)	Current (A)
	Z_{L1}	Z_{L2}	Z_{L3}	Z_{L4}	BL_1	BL_2	BL_3	BL_4	L	x_s	V_s	I_s
Value	10	10	100	200	10	10	10	10	10	5	100	0

Table 4. Parameters for the network shown in Figure 1(d).

Parameter	Load (Ω)				Length (m)					Distance (m)
	Z_{L1}	Z_{L2}	Z_{L3}	Z_{L4}	BL_1	BL_2	BL_3	BL_4	BL_5	x_s
Value	60	70	60	70	10	12	10	12	10	5
Parameter	Load (Ω)				Length (m)					Voltage (V)
	Z_{L5}	Z_{L6}	Z_{L7}	Z_{L8}	BL_6	BL_7	BL_8	BL_9	BL_{10}	V_s
Value	60	70	80	60	12	14	10	12	10	100
Parameter	Load (Ω)				Length (m)					Current (A)
	Z_{L9}	Z_{L10}	Z_{L11}		BL_{11}	L_1	L_2	L_3	L_4	I_s
Value	70	60	70		12	10	12	14	12	0

Table 5. Parameters for the network shown in Figure 1(e) and Figure 1(f).

Parameter	Load (Ω)					Length (m)							Distance (m)
	Z_{L1}	Z_{L2}	Z_{L3}	Z_{L4}	Z_{L5}	BL_1	BL_2	BL_3	BL_4	BL_5	BL_6	BL_7	x_s
Value	60	70	60	70	60	10	12	10	12	10	12	14	5
Parameter	Load (Ω)					Length (m)							voltage (V)
	Z_{L6}	Z_{L7}	Z_{L8}	Z_{L9}	Z_{L10}	BL_8	BL_9	BL_{10}	BL_{11}	BL_{12}	BL_{13}	BL_{14}	V_s
Value	70	80	60	70	60	10	12	10	12	10	10	12	100
Parameter	Load (Ω)					Length (m)							Current (A)
	Z_{L11}	Z_{L12}	Z_{L13}	Z_{L14}	Z_{L15}	BL_{15}	L_1	L_2	L_3	L_4	L_5	L_6	I_s
Value	70	60	60	70	80	14	10	12	14	12	10	12	0

**Figure 13.** Calculation results of the network shown in Figure 1(a).**Figure 14.** Calculation results of the network shown in Figure 1(b).**Figure 15.** Calculation results of the network shown in Figure 1(c).**Figure 16.** Calculation results of the network shown in Figure 1(d).

Sweeping the frequency of the excitation source from 1 Hz to 20 MHz, the comparison between the calculated results by the proposed algorithm and by the commercial software EMEC are shown in Figure 13–Figure 18. In the results figures, solid curves represent the frequency responses calculated by applying the algorithm, while dashed curves represent the results obtained from EMEC. Simulation

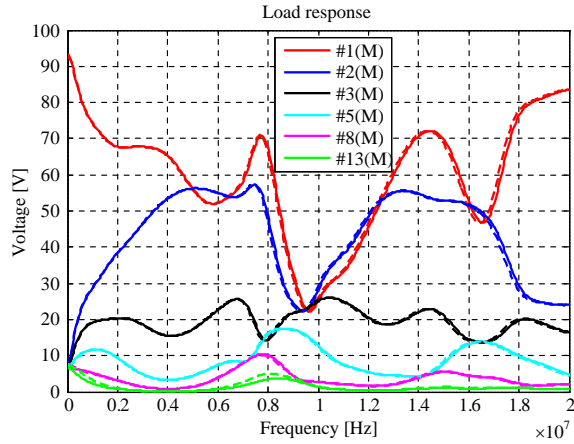


Figure 17. Calculation results of the network shown in Figure 1(e).

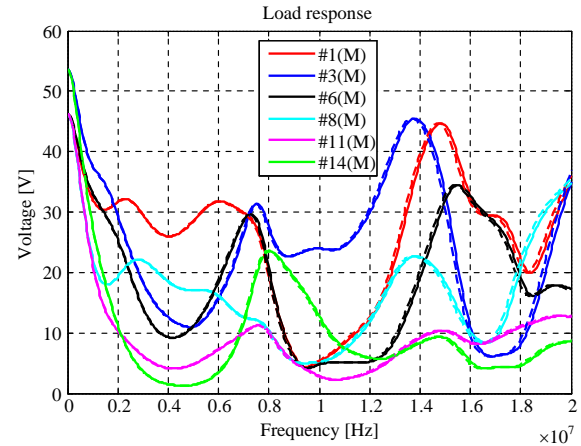


Figure 18. Calculation results of the network shown in Figure 1(f).

results show that, the frequency responses from the algorithm and the EMEC software coincide very well. This agreement shows the proposed method is accurate. The maximum error found in any studied case presented here is less than 5%.

6. CONCLUSION

We study the conventional approaches in computing the frequency responses and point out their application limitations when the power-line network grows complex. Based on the classic BLT equation, we conduct the corresponding modifications to make it applicable to the scenarios with one junction as well as multiple ends. We further propose a generic and efficient algorithm for computing the frequency responses at each load in complex power-line networks with multiple distributed junctions and branches with loads. The key idea of the algorithm is to deal the whole network with an equivalent composition of units. The reflection coefficients can be recursively achieved by regarding the units as the super loads, and the frequency responses at each load can be eventually obtained by recursively entering the units and applying the modified BLT equation locally. Results comparison shows that the algorithm converges fast and highly coincides with solutions by the EMEC software. Compared to the graphical interface based EMEC software, the proposed algorithm is much easier for the implementation as well as the adjustment of power-line network structure with various parameters.

REFERENCES

1. Anatory, J., N. Theethayi, and R. Thottappillil, "Power-line communication channel model for interconnected networks — Part I: Two-conductor system," *IEEE Trans. Power Del.*, Vol. 24, No. 1, 118–123, 2009.
2. Anatory, J., N. Theethayi, R. Thottappillil, et al., "A broadband power-line communication system design scheme for typical Tanzanian low-voltage network," *IEEE Trans. Power Del.*, Vol. 24, No. 3, 1218–1224, 2009.
3. Anatory, J., N. Theethayi, R. Thottappillil, et al., "Expressions for current/voltage distribution in broadband power-line communication networks involving branches," *IEEE Trans. Power Del.*, Vol. 23, No. 1, 188–195, 2008.
4. Anatory, J., N. Theethayi, R. Thottappillil, et al., "An experimental validation for broadband power-line communication (BPLC) model," *IEEE Trans. Power Del.*, Vol. 23, No. 3, 1380–1383, 2008.
5. Anatory, J., M. M. Kissaka, and N. H. Mvungi, et al., "Channel model for broadband power-line communication," *IEEE Trans. Power Del.*, Vol. 22, No. 1, 135–141, 2007.

6. Ding, X. and J. Meng, "Channel estimation and simulation of an indoor power-line network via a recursive time-domain solution," *IEEE Trans. Power Del.*, Vol. 24, No. 1, 144–152, 2009.
7. Shin, J., J. Lee, and J. Jeong, "Channel modeling for indoor broadband power-line communications networks with arbitrary topologies by taking adjacent nodes into account," *IEEE Trans. Power Del.*, Vol. 26, No. 3, 1432–1439, 2011.
8. Zheng, T., M. Raugi, and M. Tucci, "Time-invariant characteristics of naval power-line channels," *IEEE Trans. Power Del.*, Vol. 27, No. 2, 858–865, 2012.
9. Baum, C. E., "How to think about EMP interaction," *Proceedings of the 1974 Spring FULMEN Meeting*, 1974.
10. Baum, C. E., T. K. Liu, and F. M. Tesche, "On the analysis of general multiconductor transmission-line networks," *Interaction Note* 350, 467–547, 1978.
11. Baum, C. E., "Generalization of the BLT equation," *Proc. 13th Zurich EMC Symp.*, 131–136, 1999.
12. Tesche, F. M., "Topological concepts for internal EMP interaction," *IEEE Trans. AP*, Vol. 26, No. 1, 1978.
13. Tesche, F. M., "Development and use of the BLT equation in the time domain as applied to a coaxial cable," *IEEE Trans. EMC*, Vol. 49, No. 1, 3–11, 2007.
14. Tesche, F. M. and C. M. Butler, "On the addition of EM field propagation and coupling effects in the BLT equation," *Interaction Notes*, 2004.
15. Paul, C. R., *Introduction to Electromagnetic Compatibility*, A Wiley Interscience Publication, USA, 1992.
16. Månsson, D., R. Thottappillil, and M. Bäckström, "Propagation of UWB transients in low-voltage power installation networks," *IEEE Trans. EMC*, Vol. 50, No. 3, 619–629, 2008.
17. Carlsson, J., T. Karlsson, and G. Undén, "EMEC — An EM simulator based on topology," *IEEE Trans. EMC*, Vol. 46, No. 3, 353–358, 2004.
18. Coppersmith, D. and S. Winograd, "Matrix multiplication via arithmetic progressions," *Proceedings of the Nineteenth Annual ACM Symposium on Theory of Computing*, 1–6, 1987.
19. Pan, V., "Complexity of parallel matrix computations," *Theoretical Computer Science*, Vol. 54, No. 1, 65–85, 1987.
20. Black, P. E., "Big-O notation," *Dictionary of Algorithms and Data Structures*, 2007.
21. Mohr, A., "Quantum computing in complexity theory and theory of computation," 1–6, 2014, www.austinmohr.com/Work_files/complexity.pdf.
22. Valiant, L. G., "The complexity of computing the permanent," *Theoretical Computer Science*, Vol. 8, No. 2, 189–201, 1979.
23. Danziger, P., "Complexity of the Gaussian algorithm," Accessed: Mar. 12, 2015, Online Available: <http://www.math.ryerson.ca/danziger/professor/MTH108/Handouts/gauss-complexity.pdf>.